



Published in final edited form as:

*Circ Cardiovasc Imaging*. 2022 June ; 15(6): e013987. doi:10.1161/CIRCIMAGING.122.013987.

## Accuracy and Reproducibility of Myocardial Blood Flow Quantification by SPECT Imaging in Patients With Known or Suspected Coronary Artery Disease

Ana Carolina do A. H. de Souza, MD, PhD<sup>1</sup>,

Hendrik J. Harms, PhD<sup>1</sup>,

Laurel Martell, CNMT<sup>1</sup>,

Courtney Bibbo, CNMT<sup>1</sup>,

Meagan Harrington, CNMT<sup>1</sup>,

Kyle Sullivan, CNMT<sup>1</sup>,

Jon Hainer, BS<sup>1</sup>,

Sharmila Dorbala, MD, MPH<sup>1</sup>,

Ron Blankstein, MD<sup>1</sup>,

Viviany R. Taqueti, MD, MPH<sup>1</sup>,

Marie Foley Kijewski, PhD<sup>1</sup>,

Mi-Ae Park, PhD<sup>1</sup>,

Alejandro Meretta, MD<sup>3</sup>,

Christopher Breault, BS<sup>2</sup>,

Nathaniel Roth, PhD<sup>2</sup>,

Alexis Poitrasson-Rivière, PhD<sup>6</sup>,

Prem Soman, MD, PhD<sup>4</sup>,

Grant T. Gullberg, PhD<sup>5</sup>,

Marcelo F. Di Carli, MD<sup>1</sup>

<sup>1</sup>Cardiovascular Imaging Program, Departments of Medicine and Radiology, Brigham and Women's Hospital, Boston, MA

<sup>2</sup>Spectrum Dynamics Medical, Caesarea, Israel

<sup>3</sup>Instituto Cardiovascular Buenos Aires, Buenos Aires, Argentina

**Correspondence to:** Marcelo F. Di Carli, MD, Brigham & Women's Hospital, 75 Francis St, ASB-L1 037C, Boston, MA 02115., Phone: 617-732-6291, mdicarli@bwh.harvard.edu.

### Disclosures

Sharmila Dorbala: Research grants and consulting fees from Pfizer and GE.

Ron Blankstein: Research support from Amgen Inc and Astellas Pharma.

Prem Soman: Research Grants from Astellas Pharma and Pfizer, Consulting fees from Pfizer, Alnylam, and Eidos.

Christopher Breault: Employee of Spectrum Dynamics.

Nathaniel Roth: Employee of Spectrum Dynamics.

Alexis Poitrasson-Rivière: Employee of INVIA Medical Imaging Solutions

Marcelo F. Di Carli: Research grants from Gilead Sciences and Spectrum Dynamics (see source of funding), and consulting fees from Bayer and Janssen.

Others: none

<sup>4</sup>University of Pittsburgh, Pittsburgh, PA

<sup>5</sup>University of California at San Francisco, San Francisco, CA

<sup>6</sup>INVIA Medical Imaging Solutions, Michigan, MI

## Abstract

**Background:** Single photon emission computed tomography (SPECT) has limited ability to identify multivessel and microvascular coronary artery disease (CAD). Gamma cameras with cadmium zinc telluride (CZT) detectors allow the quantification of absolute myocardial blood flow (MBF) and flow reserve (MFR). However, evidence of its accuracy is limited and of its reproducibility is lacking. We aimed to validate <sup>99m</sup>Tc-sestamibi SPECT MBF and MFR using standard and spline-fitted reconstruction algorithms compared to <sup>13</sup>N-ammonia PET in a cohort of patients with known or suspected CAD and to evaluate the reproducibility of this technique.

**Methods:** Accuracy was assessed in thirty four participants who underwent dynamic <sup>99m</sup>Tc-sestamibi SPECT and <sup>13</sup>N-ammonia PET and reproducibility in fourteen participants who underwent two <sup>99m</sup>Tc-sestamibi SPECT studies, all within two weeks. A rest/pharmacological stress single-day SPECT protocol was performed. SPECT images were reconstructed using a standard ordered subset expectation maximization (OSEM) algorithm with (N=21) and without (N=30) application of spline fitting. SPECT MBF was quantified using a net retention kinetic model and MFR was derived as the stress/rest MBF ratio.

**Results:** SPECT global MBF with splines showed good correlation with <sup>13</sup>N-ammonia PET ( $r=0.81$ ,  $p<0.001$ ) and MFR estimates ( $r=0.74$ ,  $p<0.001$ ). Correlations were substantially weaker for standard reconstruction without splines ( $r=0.61$ ,  $p<0.001$  and  $r=0.34$ ,  $p=0.07$ , for MBF and MFR, respectively). Reproducibility of global MBF estimates with splines in paired SPECT scans was good ( $r=0.77$ ,  $p<0.001$ ), while OSEM without splines led to decreased MBF ( $r=0.68$ ,  $p<0.001$ ) and MFR correlations ( $r=0.33$ ,  $p=0.3$ ). There were no significant differences in MBF or MFR between the two reproducibility scans independently of reconstruction algorithm ( $p>0.05$  for all).

**Conclusions:** MBF and MFR quantification using <sup>99m</sup>Tc-sestamibi CZT SPECT with spatiotemporal spline fitting improved the correlation with <sup>13</sup>N-ammonia PET flow estimates and test/re-test reproducibility. The use of splines may represent an important step towards standardization of SPECT flow estimation.

## Keywords

Single photon emission computed tomography; myocardial blood flow; myocardial flow reserve; positron emission tomography

## Subject terms:

Single-Photon Emission Computerized Tomography; Positron-Emission Tomography; Gamma Cameras; Myocardial Perfusion Imaging

## INTRODUCTION

Semi-quantitative evaluation of regional myocardial perfusion has been standard practice with radionuclide myocardial perfusion imaging (MPI) for more than four decades. This approach has proven to be accurate and reproducible, with total perfusion deficit serving as a powerful marker of clinical risk and a clinically relevant guide to patient management. However, it is well recognized that this approach often underestimates the extent of ischemia in the setting of multivessel coronary artery disease (CAD)<sup>1</sup> and is not sensitive for identification of coronary microvascular dysfunction (CMD), a frequent source of chest pain worldwide, especially in the rapidly growing segment of the population with cardiometabolic risk factors<sup>2</sup>.

Quantitative measures of myocardial blood flow (MBF) and flow reserve (MFR) provide an objective and accurate means to improve the detection of angiographic CAD and characterization of its physiologic severity. MFR is now an established non-invasive quantitative marker of cardiovascular risk allowing improved risk stratification of patients with suspected or known CAD<sup>3</sup>. These quantitative measures of MBF and MFR can be determined accurately and reproducibly by positron emission tomography (PET)<sup>4,5</sup>. There is also growing evidence that single photon emission computed tomography (SPECT) using gamma cameras with cadmium zinc telluride (CZT) detectors may be used for MBF quantification<sup>6-8</sup>. However, there are limited data supporting its accuracy, and data on the reproducibility of this method are still lacking. We designed this prospective investigation to determine the accuracy of <sup>99m</sup>Tc-sestamibi CZT SPECT MBF and MFR quantification using standard and spline-fitted reconstruction algorithms compared to <sup>13</sup>N-ammonia PET, and to evaluate the test/re-test reproducibility of this technique in patients with known or suspected CAD.

## METHODS

### Study sample

Study participants were selected from the pool of patients with known or suspected CAD referred for myocardial perfusion SPECT at Brigham and Women's Hospital (Boston, MA) from February 2016 to January 2018. We also recruited healthy volunteers with a low likelihood of obstructive CAD based on the absence of symptoms, cardiovascular risk factors or history of cardiovascular disease. Study participants were assigned to two different groups for the validation and reproducibility studies (Figure 1). Individuals with suspected acute coronary syndrome, documented uncontrolled hypertension (>200/120 mmHg) within 30 days, significant cardiac arrhythmias or valvular disease, lung disease with active wheezing, decompensated heart failure, known hypersensitivity to regadenoson and pregnant or breastfeeding women were excluded. The study was approved by the Mass General Brigham Healthcare Institutional Review Board and conducted in accordance with institutional guidelines. All participants signed written informed consent. The data that support the findings of this study are available from the corresponding author upon reasonable request.

## Study design

All participants had two hospital visits. All participants in the validation group underwent rest and stress  $^{99m}\text{Tc}$ -sestamibi SPECT followed by a  $^{13}\text{N}$ -ammonia PET scan within two weeks. In the reproducibility group, participants underwent two SPECT studies also within a two-week interval for test/re-test assessment of MBF and MFR. For radiation dosimetry safety reasons, participants in the reproducibility group were different than those included in the validation group.

A total of 50 participants were initially recruited and underwent the study protocol, with 35 assigned to the validation group and 15 to the reproducibility group. One participant was excluded from the validation cohort and one participant was excluded from the reproducibility cohort due to technical problems with image acquisition which precluded further reconstruction. The validation cohort included 33 participants with known or suspected CAD and one healthy volunteer (N=34), and the reproducibility group included twelve participants with known or suspected CAD and two healthy volunteers (N=14). Due to loss of the raw data and corresponding reconstructions in both cohorts, a reduced number of study scans was available for analyses per cohort and per reconstruction algorithms compared (standard ordered subset expectation maximization (OSEM) with and without spline fitting). From the 34 scans obtained in the validation cohort, 21 were available for reconstruction using OSEM with splines, while 31 were available for reprocessing using OSEM without splines. One additional participant was identified as an outlier due to highly abnormal flow estimates obtained with OSEM without splines and was excluded. Therefore, 30 scans were available for analysis in the OSEM without splines subgroup. In the reproducibility cohort, 12 of the 14 scans were available for reconstruction with conventional OSEM without splines algorithm, while all 14 could be processed using splines. A comprehensive summary of the study sample and analyzed data is visually demonstrated in Figure S1. Baseline characteristics of the population according to available imaging reconstruction are listed in the Table S1.

## $^{99m}\text{Tc}$ -sestamibi SPECT

All participants in the validation and reproducibility groups underwent a one-day, rest/stress myocardial perfusion SPECT using a dedicated cardiac camera with solid-state cadmium zinc telluride detectors (D-SPECT<sup>®</sup>, Spectrum Dynamics Medical, Cesarea, Israel). They were instructed to abstain from caffeine, methylxanthine-containing substances and medication for at least 24 hours before the scan. MPI was performed at rest and peak vasodilator stress with regadenoson using  $^{99m}\text{Tc}$ -sestamibi as the radiotracer. Rest and stress imaging were performed in the supine position. To enable positioning of the heart in the camera's field of view, a prescan of 60 seconds was performed after injection of approximately 1 mCi. Rest listmode imaging was started simultaneously with bolus injection of  $^{99m}\text{Tc}$ -sestamibi (~6 mCi) and continued for six minutes. Gated rest images were acquired immediately after dynamic imaging for nine minutes. Approximately 30 minutes after completion of the rest images, intravenous regadenoson (0.4 mg) was infused over 30 seconds. Thirty seconds after completion of the regadenoson administration, a second dose of  $^{99m}\text{Tc}$ -sestamibi (~22 mCi) was injected and listmode imaging was recorded in the same manner. Gated stress images were obtained immediately for approximately 7

minutes. Heart rate (HR) (in bpm), systemic blood pressure (BP) (in mmHg), and 12-lead electrocardiogram were recorded at baseline and every minute during and after regadenoson administration (Table S2). Radiotracer delivery was performed with an automatic injector to guarantee injection reproducibility.

Rest and stress list mode images were reformatted into 32 frames (21×3-sec, 1×9-sec, 1×15-sec, 1×21-sec, 1×27-sec and 7×30-sec frames) and reconstructed using a standard ordered subset expectation maximization (OSEM) algorithm with spline fitting (7 iterations and 32 subsets) and without spline fitting (4 iterations and 32 subsets). Spline fitting of dynamic SPECT data was performed by fitting linear 3<sup>rd</sup> degree temporal functions with geometrically increasing knot spacing to the time-activity curves (TACs), as previously described<sup>9,10</sup>. The same voxel model was maintained in the standard OSEM reconstruction. Since the spline model is linear, we used the standard OSEM solver with minor modifications.

For both reconstruction approaches, automated regions of interest (ROI) were placed and copied along the entire dynamic series to obtain arterial and myocardial tissue TACs using commercially available software (Corridor4DM, INVIA Medical Imaging Solutions, Ann Arbor, Michigan). Motion correction was applied to each frame after visual inspection and manual image alignment to the left ventricular (LV) contours in the short and long axis planes using the same software. LV contours were automatically generated from myocardial images summed from two minutes to the end of the acquisition. Partial volume correction was applied using the same software. For this correction, 0.63 was derived from having a resolution of 11mm and a myocardium width of 10mm. Attenuation and scatter correction were not performed, but we conducted a phantom study to assess the biases in global and regional retention and myocardial perfusion reserve index (MPR index) estimates due to (1) scatter from liver activity and (2) lack of attenuation correction. The results are provided in the Supplemental materials (Tables S3 and S4). The residual radioactivity from the rest injection was subtracted from the stress dynamic series<sup>11</sup>, and prescan injection was not subtracted from rest series. TACs were then fitted with a net retention kinetic model, corrected for the <sup>99m</sup>Tc-sestamibi extraction fraction in order to obtain regional and global MBF values (mL/min/g) using the Renkin-Crone extraction fraction model (a=0.899, b=0.541). Rest MBF was normalized for rate pressure product (RPP), calculated as the product of HR and systolic BP. MFR was calculated as the ratio of stress MBF to normalized rest MBF.

Semiquantitative expert visual interpretation of myocardial perfusion images was performed using a 17-segment model and standard five-point system<sup>12</sup>. Summed rest (SRS), stress (SSS), and difference scores (SDS) were computed to reflect scar, scar plus ischemia and ischemia, respectively<sup>12</sup>.

### **<sup>13</sup>N-ammonia PET**

Participants in the validation cohort were imaged in a whole-body PET scanner (Discovery RX or STE LightSpeed 64, GE Healthcare, Milwaukee, WI). They were instructed to fast overnight and refrain from caffeine and methylxanthine-containing substances or vasoactive drugs for 24 hours. MBF was measured at rest and during peak vasodilator stress with

regadenoson using  $^{13}\text{N}$ -ammonia as the flow tracer, as previously described<sup>4</sup> (Supplemental materials).

Regional and global rest and stress MBF was obtained by fitting TACs to a previously validated two-compartment kinetic model<sup>7</sup> using commercially available software (Corridor4DM, INVIA Medical Imaging Solutions, Ann Arbor, Michigan). Regional and global MFR were calculated as the ratio of stress to normalized rest MBF. PET semiquantitative visual interpretation was performed as described for SPECT. An index of coronary vascular resistance (CVR) at rest and stress was calculated by dividing the corresponding mean arterial pressure by MBF for both SPECT and PET data.

### Statistical analyses

Continuous variables were expressed as mean and standard deviation (SD) or median and interquartile range (IQR). Categorical variables were expressed as rates with percentages (%). Spearman correlation was used to describe the association between  $^{13}\text{N}$ -ammonia PET and  $^{99\text{m}}\text{Tc}$ -sestamibi SPECT estimates of MBF and MFR in the validation cohort, with and without spline fitting added to OSEM standard reconstruction. Bland-Altman plots of the residuals (difference between MBF and MFR values obtained from SPECT and PET studies in the validation cohort or between the two sequential SPECT studies in the reproducibility cohort) against the means were constructed to evaluate agreement and assess for systematic errors or bias. Wilcoxon signed-ranks test was performed to compare paired MBF and MFR estimates in the validation and reproducibility cohorts. For the latter, mean percentage difference (%) between MBF and MFR estimates was calculated as the absolute value change divided by the average of the two sequential measurements obtained within two weeks, multiplied by 100. The intra-class correlation coefficient (ICC) was also calculated for the rest and stress MBF and the MFR data. A two-sided p-value <0.05 was considered statistically significant. Analyses were performed using IBM SPSS version 23.0 (IBM Statistics, Armonk, NY, USA).

## RESULTS

### Study sample

Table 1 summarizes the characteristics of the final study sample. The median age was 63 (52-72) years, 52.1% were female and 81.3% were white, with similar distributions between the validation and reproducibility cohorts. The most frequent cardiovascular risk factors were hypertension (83.3%) and dyslipidemia (72.9%). In the validation cohort, semiquantitative visual analysis identified 31 patients with a normal scan by SPECT and 26 by PET. In the reproducibility cohort, one patient had an abnormal scan.

### Systemic hemodynamics and radiotracer doses

Systemic hemodynamics and administered radiotracer doses for the two study groups are presented in Table S2. In the reproducibility cohort, HR, systolic, diastolic and mean arterial BP at rest and stress were comparable between the two SPECT scans. In the validation cohort, rest systolic, diastolic and mean arterial BP, as well as peak diastolic BP and mean arterial BP were significantly higher at the SPECT scan visit compared to the PET visit.



## Accuracy of $^{99m}\text{Tc}$ -sestamibi SPECT estimates of MBF and MFR compared to $^{13}\text{N}$ -ammonia PET

**OSEM SPECT reconstruction**—OSEM reconstructions of the SPECT data were available in 31 of the 34 patients in the validation cohort. One participant was identified as an outlier due to highly abnormal global MBF and MFR values and was excluded. Therefore, 30 scans were available for analyses.

Table 2 shows the mean global MBF and MFR values for participants in the validation cohort. Uncorrected and RPP-corrected rest global MBF were not significantly different between SPECT and PET. However, stress MBF and MFR were significantly higher with SPECT as compared to PET. To account for the higher BP during the SPECT study visit, we calculated an index of coronary vascular resistance and found that hyperemic CVR was similar for both SPECT and PET, suggesting that differences in MBF were not related to changes in BP between the two studies. Global rest and stress MBF by  $^{99m}\text{Tc}$ -sestamibi SPECT and  $^{13}\text{N}$ -ammonia PET showed a moderate correlation ( $r=0.61$ ,  $p<0.001$ ) (Figure 2A). Bland-Altman plots showed an overestimation of MBF by SPECT ( $0.26\pm 0.76$  mL/min/g, with 1.75 to  $-1.24$  mL/min/g as 95% limits of agreement [mean difference  $\pm 1.96$  SD]) (Figure 2B). This overestimation was predominantly driven by an overestimation of stress MBF, as seen graphically. The correlation of global MFR estimates between SPECT and PET was poor and non-significant ( $r=0.34$ ,  $p=0.07$ ) (Figure 2C). Bland-Altman plots showed an overestimation of MFR by SPECT compared to PET, with a mean difference of  $0.45\pm 0.94$  and 2.29 to  $-1.39$  as limits of agreement (Figure 2D).

**OSEM with spline fitting SPECT reconstruction**—Overall, 21 of the 34 SPECT studies were available for reprocessing using spline fitting. Rest and peak stress MBF were significantly lower with SPECT compared to PET. Hyperemic CVR was higher in the subgroup with spline reconstructions. However, MFR estimates were comparable between the two modalities ( $p>0.05$ ). Addition of spline fitting to the reconstruction led to a significant improvement in the correlation between SPECT and PET MBF ( $r=0.81$ ,  $p<0.001$ ) (Figure 3A) and CVR estimates ( $r=0.79$ ,  $p<0.001$ ) (Figure S2). Bland-Altman plots revealed an overall underestimation of MBF by SPECT, with a mean difference of  $-0.24\pm 0.33$  mL/min/g and narrower limits of agreement (0.41 to  $-0.88$  mL/min/g) when compared to conventional OSEM reconstruction without splines (Figure 3B). Likewise, addition of spline fitting led to a marked improvement in the correlation between SPECT and PET estimates of MFR ( $r=0.75$ ,  $p<0.001$ ) (Figure 3C) with slight overestimation of MFR by SPECT (mean difference  $0.17\pm 0.5$ ) and significantly narrower limits of agreement (1.15 to  $-0.81$ ) (Figure 3D), as compared to conventional OSEM reconstruction.

In sensitivity analyses including only the 18 participants who had both reconstructions available, we observed a modest improvement in MBF correlations between PET and SPECT with standard OSEM ( $r=0.73$ ,  $p<0.001$ ) whereas results remained unchanged for the spline-fitted data (Figures S3 and S4).

**Regional MBF and MFR measurements using OSEM and OSEM with spline fitting SPECT reconstructions**—There was a moderate correlation between PET and

SPECT regional MBF estimates with conventional OSEM reconstruction without splines (N=90 territories;  $r=0.59$ ,  $p<0.001$ ), with a mean difference of 0.35 mL/min/g (Figure S5). Similarly to the results observed for global MBF, addition of spline fitting led to an improved correlation between SPECT and PET-derived MBF, although still moderate (N=63 territories;  $r=0.69$ ,  $p<0.001$ ). Bland-Altman plots revealed a mean difference of  $-0.18$  mL/min/g, with 0.65 and  $-1.00$  as limits of agreement, which were considerably narrower than the ones observed with OSEM reconstruction without splines. Consistent with the global findings, regional MBF and MFR estimates obtained with SPECT using OSEM reconstruction without splines were significantly higher as compared to PET, while the addition of splines led to an overall underestimation of rest and stress MBF (Table S5).

### Reproducibility of $^{99m}\text{Tc}$ -sestamibi SPECT estimates of MBF and MFR

Table 3 shows MBF and MFR estimates from two consecutive  $^{99m}\text{Tc}$ -sestamibi SPECT studies performed in the reproducibility cohort. Overall, 12 of the 14 scans were available for reconstruction with the conventional OSEM algorithm, while all 14 could be processed using splines. There were no significant differences between global rest, stress, MFR, and RPP-normalized MFR measurements between the two scans, independently of reconstruction algorithm ( $p>0.05$  for all). Mean percentage differences (%) between scans ranged from 0.7% to 5.0% for conventional OSEM without splines and from 1.4% to 7.6% for OSEM with splines. The ICC for OSEM without splines reconstruction was 0.77, 0.89, and 0.53 for rest MBF, stress MBF and MFR, respectively, whereas the corresponding values after adding splines were 0.75, 0.71 and 0.76. Figure 4 shows a significant correlation for global rest and stress MBF between the two scans with the spline-fitted OSEM reconstruction ( $r=0.77$ ,  $p<0.001$ ), while MFR correlations were slightly worse for global MFR ( $r=0.63$ ,  $p=0.017$ ). The corresponding Bland-Altman plot shows no systematic errors, with the major proportion of MBF differences remaining within the 95% limits of agreement. Importantly, the adoption of conventional OSEM without splines reconstruction led to a decreased MBF correlation ( $r=0.68$ ,  $p<0.001$ ) and a non-significant MFR correlation ( $r=0.33$ ,  $p=0.3$ ) between the two scans (Figure S6).

The correlation between regional rest and stress MBF was good with the use of splines ( $r=0.71$ ,  $p<0.001$ ) (Figure S7). Although conventional OSEM also led to a positive, significant correlation between regional MBF values ( $r=0.68$ ,  $p<0.001$ ), it was associated with decreased agreement between the two sequential scans.

## DISCUSSION

SPECT has played a critical role in the evaluation of patients with suspected or known CAD for nearly 50 years. Despite its wide availability, the spatially relative nature of myocardial perfusion images limits the evaluation of individuals with multivessel CAD, diffuse atherosclerosis and/or coronary microvascular dysfunction (CMD). This is important because diffuse atherosclerosis and CMD are prevalent, especially among patients with cardiometabolic disease, and both are drivers of increased clinical risk<sup>3,13</sup>. Absolute estimation of MBF and MFR helps to overcome this limitation and allows more precise



quantification of myocardial ischemia, thereby enhancing risk stratification and patient management.

Our results confirm the technical feasibility of MBF quantification using  $^{99m}\text{Tc}$ -sestamibi SPECT and expands the current knowledge in two important ways. First, by demonstrating that applying spline fitting to CZT SPECT reconstruction improves signal-to-noise in dynamic series and increases the accuracy of flow estimates when compared to  $^{13}\text{N}$ -ammonia PET myocardial perfusion imaging. Indeed, spline fitting of the rest and stress myocardial perfusion data resulted in a substantially improved correlation and reduced mean difference between CZT SPECT and PET MBF and MFR estimates as compared to standard OSEM. Nonetheless, the agreement between SPECT and PET flows worsened during stress using both reconstruction algorithms but was especially marked with standard OSEM, as similarly observed in prior work using the same scanner<sup>7</sup>. Using imprecision analysis and clinical simulations, a recent study reported SPECT MFR imprecision across previously published validation studies - defined as the standard deviation of the mean difference between SPECT and PET MFR - to range from 0.556 to 0.829<sup>14</sup>. Accordingly, our results are consistent with previous investigations of SPECT MFR quantification<sup>7,11,15,16</sup>, and reflect a significant reduction in MBF and MFR imprecision with spline fitting application.

The effect of spatiotemporal spline fitting is particularly important for the early frames of dynamic reconstruction due to the rapid changes in tracer distribution and facilitates segmentation of arterial blood and myocardial tissue counts, likely reducing partial volume effects and improving the accuracy of the arterial input function<sup>10,17,18</sup>. As spatiotemporal splines are used to model the dynamic distribution of the radiopharmaceutical within the volume of interest from the projected field of view<sup>17</sup> and allow for the extraction of kinetic parameters directly from dynamic projections, they can minimize bias and noise<sup>9,10,19</sup>. The improved accuracy with spline fitting is consistent with prior work using conventional SPECT systems<sup>20</sup>, as it uses count statistics from all projections and weights their contributions using linear sums of basis functions, which reduces the frame-to-frame variations in TACs, while the OSEM reconstruction only uses projections from a single angle. Therefore, splines provide smooth TACs for segmented myocardial volumes throughout a continuous period of time and may represent a novel advance for the standardization and implementation of CZT SPECT-derived MBF and MFR into clinical practice.

Second, our study is the first to assess the test/re-test reproducibility of MBF and MFR estimates using  $^{99m}\text{Tc}$ -sestamibi SPECT in a dedicated cardiac CZT camera. Our results show that this methodology is reproducible, resulting in mean MBF and MFR differences below 10% between studies performed within two weeks of each other. These results are consistent with previous  $^{82}\text{Rb}$  and  $^{13}\text{N}$ -ammonia PET assessments of flow reproducibility<sup>4,21</sup>. Importantly, the test-retest variability was markedly improved by the application of splines when compared to standard reconstruction alone. These results further support their role in reducing the inherent statistical noise from SPECT dynamic series. Despite showing higher test-retest imprecision than previously described for  $^{82}\text{Rb}$  PET<sup>14,22</sup>, our results show modest improvement relative to recently published precision assessment of MBF repeatability with a cardiac CZT camera using  $^{99}\text{Tc}$ -tetrofosmin<sup>23</sup>.

Despite the significant imprecision reduction in MBF and MFR estimation with spline fitting, the relatively limited degree of correlation between SPECT and PET flows can be explained by different factors. First, SPECT  $^{99m}\text{Tc}$  radiotracers show lower extraction fraction at high flows, which negatively impacts MBF quantification during stress and requires the use of correction models. Second, although solid state cameras have increased photon sensitivity and resolution compared to traditional sodium-iodide cameras, image quality is still relatively inferior to that of PET systems. Furthermore, most currently available CZT SPECT systems, unlike PET, are not hybrid and do not allow for CT-based attenuation correction. Third, dynamic SPECT processing still largely relies on manual motion correction, which represents an additional source of flow variability. Finally, differences in radiotracer selection, injected doses, reconstruction algorithms and kinetic models lead to the significant heterogeneity of flow values obtained with CZT SPECT in previous studies.

The findings of this study have to be interpreted in light of some limitations. First, this is a single-center experience with a relatively modest sample size. However, the study has a balanced inclusion of overweight or obese men and women with multiple risk factors, which adequately represents patients undergoing SPECT MPI. OSEM and spline-fitted reconstructions were unfortunately not available for every patient in the study due to loss of raw data. However, there were no differences between the characteristics of patients with and without spline-fitted data, especially with respect to sex, BMI, or injected dose. Second, our objective was to assess the accuracy and reproducibility of flow quantification with CZT SPECT when compared to PET and, thus, our study design did not include a requirement of referral to coronary angiography. The accuracy of our quantitative approach for detecting multivessel CAD will have to be tested. Third, we did not perform individual attenuation or scatter correction of the SPECT data. Although some studies have suggested that the use of AC do not significantly improve the accuracy of SPECT MBF and MFR over PET<sup>11,24</sup>, or even the test-retest repeatability of flow estimates<sup>23</sup>, the need of AC remains to be confirmed by larger clinical studies. Similarly, since the initial positioning dose was not subtracted from the rest series, its effects on flow estimation also remain to be investigated. Fourth, we applied short frame duration (3-seconds) during the first minute to capture blood phase and avoid averaging of bolus and myocardial phases. This frame duration has been previously validated in other studies<sup>7,16</sup>, but the optimal frame duration still needs to be determined. Additionally, the implementation of validated, fully automated motion correction algorithms holds the potential to increase accuracy and reproducibility of CZT SPECT-derived MFR even further. This technique may become of special relevance in sites where PET is not available due to economical or logistical reasons.

## CONCLUSION

Myocardial blood flow (MBF) and flow reserve (MFR) quantification using  $^{99m}\text{Tc}$ -sestamibi CZT SPECT with spatiotemporal spline fitting reconstruction significantly improved the correlation with  $^{13}\text{N}$ -ammonia PET flow estimates and test/re-test reproducibility. The use of splines may represent an important step towards standardization of CZT SPECT flow estimation.

## Supplementary Material

Refer to Web version on PubMed Central for supplementary material.

## Acknowledgments

All the authors have made substantial contributions to the study design, data collection, analysis and drafting and/or editing of the manuscript. All the authors have access to the data and approved to be named as authors in the manuscript.

## Sources of Funding

The study was supported by an investigator-initiated, institutional grant from Spectrum Dynamics.

## NON-STANDARD ABBREVIATIONS AND ACRONYMS

<b>CAD</b>	coronary artery disease
<b>CMD</b>	coronary microvascular dysfunction
<b>CZT</b>	cadmium zinc telluride
<b>MBF</b>	myocardial blood flow
<b>MFR</b>	myocardial flow reserve
<b>MPI</b>	myocardial perfusion imaging
<b>OSEM</b>	ordered subset expectation maximization
<b>PET</b>	positron emission tomography
<b>ROI</b>	region of interest
<b>SPECT</b>	single photon emission computed tomography
<b>TAC</b>	time-activity curve

## REFERENCES

1. Lima RSL, Watson DD, Goode AR, Siadaty MS, Ragosta M, Beller GA, Samady H. Incremental value of combined perfusion and function over perfusion alone by gated SPECT myocardial perfusion imaging for detection of severe three-vessel coronary artery disease. *J Am Coll Cardiol.* 2003;42:64–70. [PubMed: 12849661]
2. Taqueti VR, Di Carli MF. Coronary Microvascular Disease Pathogenic Mechanisms and Therapeutic Options: JACC State-of-the-Art Review. *J Am Coll Cardiol.* 2018;72:2625–2641. [PubMed: 30466521]
3. Murthy VL, Naya M, Foster CR, Hainer J, Gaber M, Di Carli G, Blankstein R, Dorbala S, Sitek A, Pencina MJ, et al. Improved cardiac risk assessment with noninvasive measures of coronary flow reserve. *Circulation.* 2011;124:2215–2224. [PubMed: 22007073]
4. El Fakhri G, Kardan A, Sitek A, Dorbala S, Abi-Hatem N, Lahoud Y, Fischman A, Coughlan M, Yasuda T, Di Carli MF. Reproducibility and Accuracy of Quantitative Myocardial Blood Flow Assessment with 82Rb PET: Comparison with 13N-Ammonia PET. *J Nucl Med.* 2009;50:1062–1071. [PubMed: 19525467]
5. Murthy VL, Bateman TM, Beanlands RS, Berman DS, Borges-Neto S, Chareonthaitawee P, Cerqueira MD, DeKemp RA, Gordon DePuey E, Dilsizian V, et al. Clinical quantification of

myocardial blood flow using PET: Joint position paper of the SNMMI cardiovascular council and the ASNC. *J Nucl Med*. 2018;59:273–293. [PubMed: 29242396]

6. Ben-Haim S, Murthy VL, Breault C, Allie R, Sitek A, Roth N, Fantony J, Moore SC, Park M-A, Kijewski M, et al. Quantification of Myocardial Perfusion Reserve Using Dynamic SPECT Imaging in Humans: A Feasibility Study. *J Nucl Med*. 2013;54:873–879. [PubMed: 23578996]
7. Agostini D, Roule V, Nganoa C, Roth N, Baavour R, Parienti J-J, Beygui F, Manrique A. First validation of myocardial flow reserve assessed by dynamic 99mTc-sestamibi CZT-SPECT camera: head to head comparison with 15O-water PET and fractional flow reserve in patients with suspected coronary artery disease. The WATERDAY study. *Eur J Nucl Med Mol Imaging*. 2018;45:1079–1090. [PubMed: 29497801]
8. de Souza ACAH, Gonçalves BKD, Tedeschi AL, Lima RSL. Quantification of myocardial flow reserve using a gamma camera with solid-state cadmium-zinc-telluride detectors: Relation to angiographic coronary artery disease. *J Nucl Cardiol*. 2021;28:876–884. [PubMed: 31222529]
9. Reutter BW, Gullberg GT, Huesman RH. Direct least-squares estimation of spatiotemporal distributions from dynamic SPECT projections using a spatial segmentation and temporal B-splines. *IEEE Trans Med Imaging*. 2000;19:434–450. [PubMed: 11021687]
10. Reutter BW, Gullberg GT, Huesman RH. Accuracy and precision of compartmental model parameters obtained from directly estimated dynamic SPECT time-activity curves. *IEEE Trans Nucl Sci*. 2004;51:170–176.
11. Wells RG, Marvin B, Poirier M, Renaud J, DeKemp RA, Ruddy TD. Optimization of SPECT Measurement of Myocardial Blood Flow with Corrections for Attenuation, Motion, and Blood Binding Compared with PET. *J Nucl Med*. 2017;58:2013–2019. [PubMed: 28611245]
12. Berman DS, Abidov A, Kang X, Hayes SW, Friedman JD, Sciammarella MG, Cohen I, Gerlach J, Waechter PB, Germano G, et al. Prognostic validation of a 17-segment score derived from a 20-segment score for myocardial perfusion SPECT interpretation. *J Nucl Cardiol*. 2004;11:414–423. [PubMed: 15295410]
13. Bajaj NS, Osborne MT, Gupta A, Tavakkoli A, Bravo PE, Vita T, Bibbo CF, Hainer J, Dorbala S, Blankstein R, et al. Coronary Microvascular Dysfunction and Cardiovascular Risk in Obese Patients. *J Am Coll Cardiol*. 2018;72:707–717. [PubMed: 30092946]
14. Renaud JM, Poitras-Rivière A, Hagio T, Moody JB, Arida-Moody L, Ficaro EP, Murthy VL. Myocardial flow reserve estimation with contemporary CZT-SPECT and 99mTc-tracers lacks precision for routine clinical application. *J Nucl Cardiol*. 2021; DOI: 10.1007/s12350-021-02761-0
15. Giubbini R, Bertoli M, Durmo R, Bonacina M, Peli A, Faggiano I, Albano D, Milan E, Stern E, Paghera B, et al. Comparison between N13NH3-PET and 99mTc-Tetrofosmin-CZT SPECT in the evaluation of absolute myocardial blood flow and flow reserve. *J Nucl Cardiol*. 2021;28:1906–1918. [PubMed: 31728817]
16. Acampa W, Zampella E, Assante R, Genova A, De Simini G, Mannarino T, D'Antonio A, Gaudieri V, Nappi C, Buongiorno P, et al. Quantification of myocardial perfusion reserve by CZT-SPECT: A head to head comparison with 82Rubidium PET imaging. *J Nucl Cardiol*. 2021;28:2827–2839. [PubMed: 32383083]
17. Gullberg GT, Reutter BW, Sitek A, Maltz JS, Budinger TF. Dynamic single photon emission computed tomography—basic principles and cardiac applications. *Phys Med Biol*. 2010;55:R111–R191. [PubMed: 20858925]
18. Reutter BW, Gullberg GT, Huesman RH. Effects of temporal modelling on the statistical uncertainty of spatiotemporal distributions estimated directly from dynamic SPECT projections. *Phys Med Biol*. 2002;47:2673–2683. [PubMed: 12200931]
19. Winant CD, Aparici CM, Zelnik YR, Reutter BW, Sitek A, Bacharach SL, Gullberg GT. Investigation of dynamic SPECT measurements of the arterial input function in human subjects using simulation, phantom and human studies. *Phys Med Biol*. 2012;57:375–393. [PubMed: 22170801]
20. Alhassen F, Nguyen N, Bains S, Gould RG, Seo Y, Bacharach SL, Song X, Shao L, Gullberg GT, Aparici CM. Myocardial blood flow measurement with a conventional dual-head SPECT/CT with spatiotemporal iterative reconstructions - a clinical feasibility study. *Am J Nucl Med Mol Imaging*. 2013;4:53–9. [PubMed: 24380045]

21. Nagamachi S, Czernin J, Kim AS, Sun KT, Böttcher M, Phelps ME, Schelbert HR. Reproducibility of measurements of regional resting and hyperemic myocardial blood flow assessed with PET. *J Nucl Med.* 1996;37:1626–31. [PubMed: 8862296]
22. Kitkungvan D, Johnson NP, Roby AE, Patel MB, Kirkeeide R, Gould KL. Routine Clinical Quantitative Rest Stress Myocardial Perfusion for Managing Coronary Artery Disease: Clinical Relevance of Test-Retest Variability. *JACC Cardiovasc Imaging.* 2017;10:565–577. [PubMed: 28017383]
23. Wells RG, Radonjic I, Clackdoyle D, Do J, Marvin B, Carey C, DeKemp RA, Ruddy TD. Test-Retest Precision of Myocardial Blood Flow Measurements With 99m Tc-Tetrofosmin and Solid-State Detector Single Photon Emission Computed Tomography. *Circ Cardiovasc Imaging.* 2020;13:1–11.
24. Bailly M, Thibault F, Courtehoux M, Metrard G, Ribeiro MJ. Impact of attenuation correction for CZT-SPECT measurement of myocardial blood flow. *J Nucl Cardiol.* 2021;28:2560–2568. [PubMed: 32080802]
25. King M, Tsui B, Pan T. Attenuation compensation for cardiac single-photon emission computed tomographic imaging: Part 1. Impact of attenuation and methods of estimating attenuation maps. *J Nucl Cardiol.* 1995;2:513–524. [PubMed: 9420834]
26. King MA, Tsui BMW, Pan TS, Glick SJ, Soares EJ. Attenuation compensation for cardiac single-photon emission computed tomographic imaging: Part 2. Attenuation compensation algorithms. *J Nucl Cardiol.* 1996;3:55–64. [PubMed: 8799228]
27. Patton JA, Turkington TG. SPECT/CT physical principles and attenuation correction. *J Nucl Med Technol.* 2008;36:1–10. [PubMed: 18287196]

### Clinical Perspective

Myocardial flow reserve (MFR) is an established non-invasive quantitative marker of cardiovascular risk and helps to overcome the limitations of relative single photon emission computed tomography (SPECT) perfusion imaging, including the evaluation of individuals with multivessel coronary artery disease (CAD), diffuse atherosclerosis and/or coronary microvascular dysfunction. MFR can be determined using positron emission tomography (PET), but this method still has limited availability worldwide. Newer gamma cameras with cadmium zinc telluride (CZT) detectors allow the acquisition of dynamic images and quantification of MFR. We showed for the first time that the addition of spatiotemporal spline fitting to a conventional reconstruction algorithm improves the agreement between measurements of myocardial blood flow (MBF) and MFR using  $^{99m}\text{Tc}$ -sestamibi CZT SPECT in comparison to the gold standard  $^{13}\text{N}$ -ammonia PET in a cohort of patients with known or suspected CAD. We also showed that this method is reproducible and that the test-retest variability was markedly improved by the application of splines when compared to standard reconstruction alone. The application of splines represents an important step towards standardizing flow estimation with SPECT and has the potential to broaden the use of commercially available CZT gamma cameras for MFR quantification, with direct implications to risk stratification and management of the rapidly growing segment of the population with cardiometabolic risk factors.



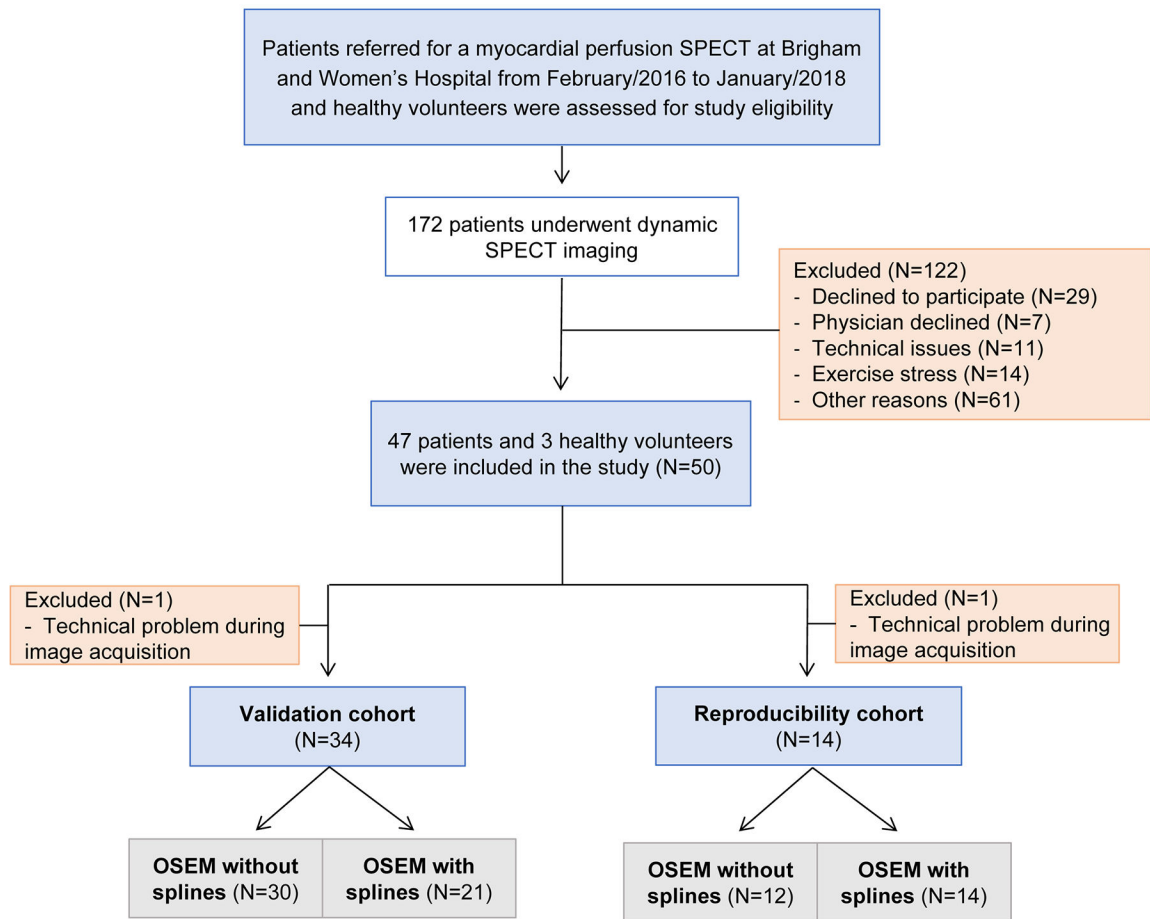


**Figure 1:**  
Flowchart of the study population

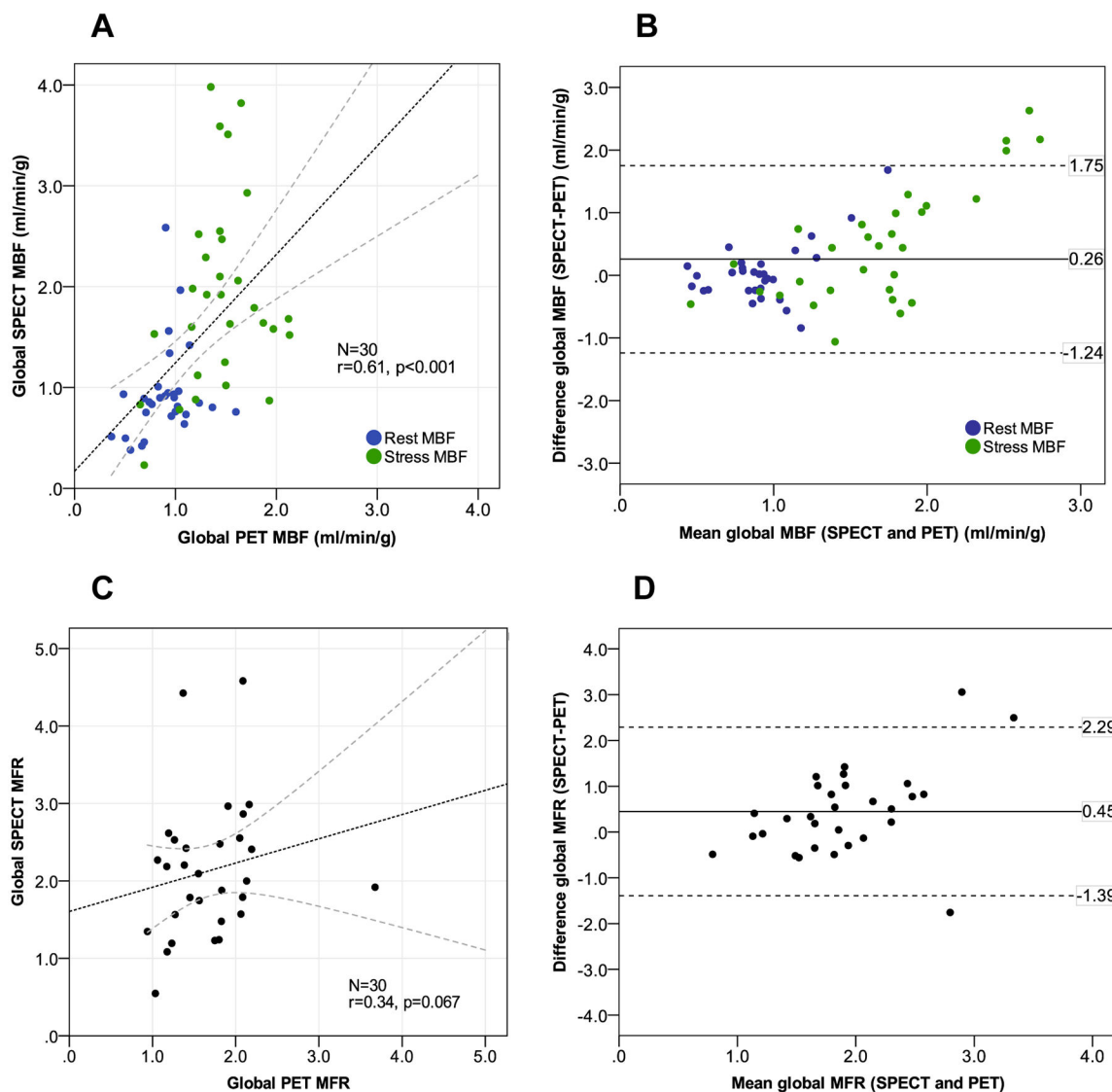


**Figure 2:** Comparison of global rest and stress myocardial blood flow (MBF) and flow reserve (MFR) estimated with  $^{13}\text{N}$ -ammonia PET and  $^{99\text{m}}\text{Tc}$ -sestamibi SPECT using standard ordered subset expectation maximization (OSEM) reconstruction without spline fitting. Correlation plots of global MBF (panel A) and MFR measurements (panel C). Bland–Altman plots of global MBF (panel B) and MFR measurements (panel D).

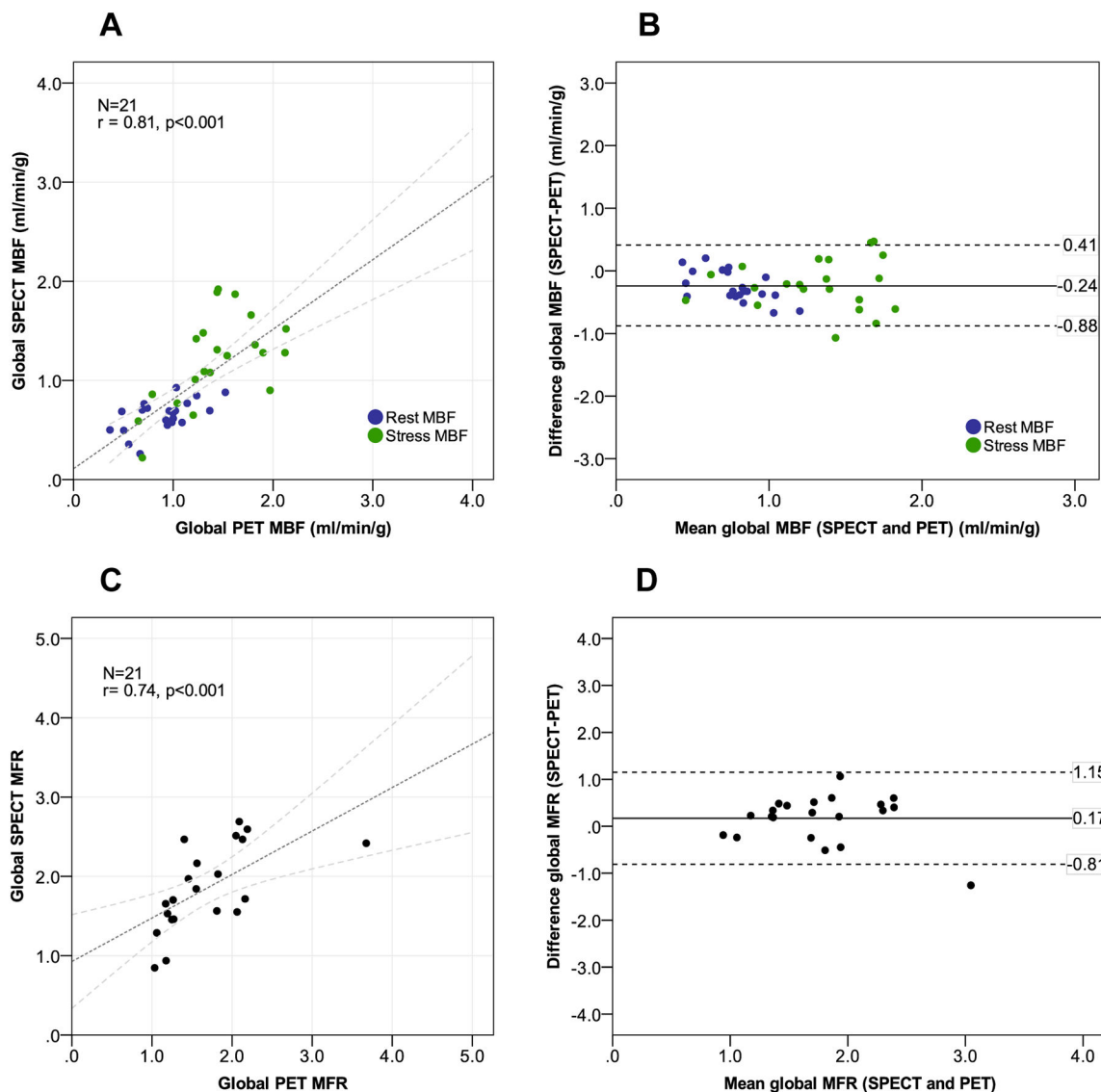


**Figure 3:** Comparison of global rest and stress myocardial blood flow (MBF) and flow reserve (MFR) estimated with  $^{13}\text{N}$ -ammonia PET and  $^{99\text{m}}\text{Tc}$ -sestamibi SPECT using standard ordered subset expectation maximization (OSEM) reconstruction with spline fitting. Correlation plots of global MBF (panel A) and MFR measurements (panel C). Bland–Altman plots of global MBF (panel B) and MFR measurements (panel D).

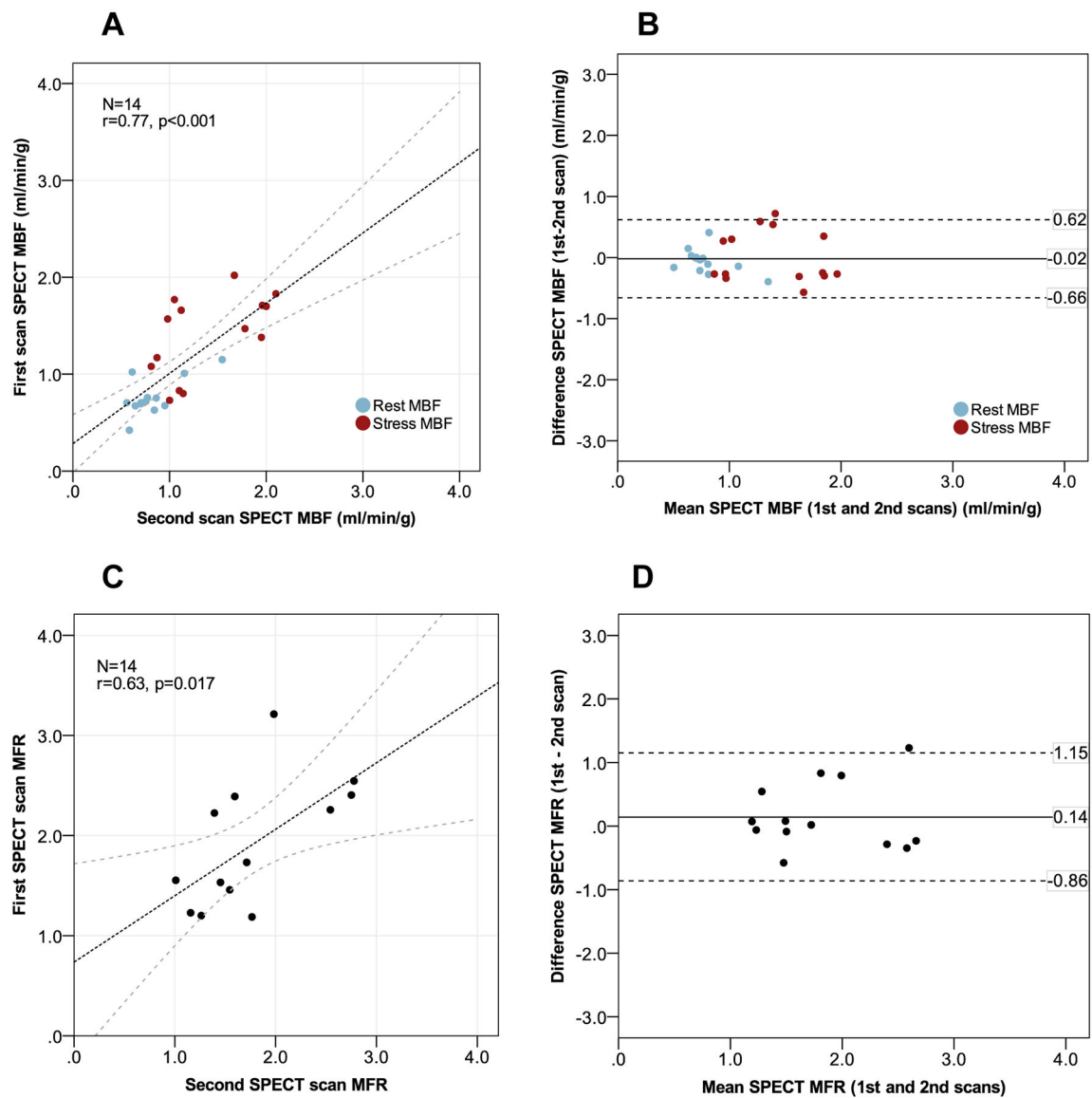


**Figure 4:**

Reproducibility analyses of global rest and stress myocardial blood flow (MBF) and flow reserve (MFR) estimated with  $^{99m}\text{Tc}$ -sestamibi SPECT within two weeks using ordered subset expectation maximization (OSEM) reconstruction with spline fitting. Correlation plots of rest and stress MBF (panel A) and MFR measurements (panel C). Bland–Altman plots of rest and stress MBF (panel B) and MFR measurements (panel D) obtained at the two visits.

**Table 1:**

Baseline characteristics of the study population

	<b>Overall cohort (N=48)</b>	<b>Validation cohort (N=34)</b>	<b>Reproducibility cohort (N=14)</b>
<b><i>Demographics</i></b>			
Age	63 (52-72)	63 (54-73)	63 (54-70)
Male sex	23 (47.9%)	17 (50%)	6 (42.9%)
White race	39 (81.3%)	28 (82.4%)	11 (78.6%)
Non-Hispanic	46 (95.8%)	32 (94.1%)	14 (100%)
BMI	30.6 (27.6-33.6)	31.1 (27.8-34.1)	28.7 (26.9-32.6)
<b><i>Clinical characteristics</i></b>			
History of known CAD	13 (27.1%)	11 (32.4%)	2 (14.3%)
Family history of known CAD	17 (35.4%)	12 (35.3%)	5 (35.7%)
Hypertension	40 (83.3%)	30 (88.2%)	10 (71.4%)
Dyslipidemia	35 (72.9%)	25 (73.5%)	10 (71.4%)
Diabetes mellitus	12 (25%)	9 (26.5%)	3 (21.4%)
Current smoker	6 (12.5%)	2 (5.9%)	4 (28.6%)
Previous MI or acute coronary syndrome	9 (18.8%)	7 (20.6%)	2 (14.3%)
Revascularization history (PCI/CABG)	9 (18.8%)	7 (20.6%)	2 (14.3%)
History of stroke or transient ischemic attack	2 (4.2%)	1 (2.9%)	1 (7.1%)
Peripheral artery disease	7 (14.6%)	5 (14.7%)	2 (14.3%)
<b><i>Medications</i></b>			
Beta-blockers	25 (52.1%)	20 (58.8%)	5 (35.7%)
ACE inhibitors	16 (33.3%)	12 (35.3%)	4 (28.6%)
ARB	9 (18.8%)	7 (20.6%)	2 (14.3%)
Statins	31 (64.6%)	23 (67.6%)	8 (57.1%)
Nitroglycerin	6 (12.5%)	4 (11.8%)	2 (14.3%)
Antiplatelet therapy	17 (35.4%)	11 (32.4%)	6 (42.9%)
Anticoagulation	7 (14.6%)	7 (20.6%)	0 (0%)
Diuretics	17 (35.4%)	14 (41.2%)	3 (21.4%)
Insulin	5 (10.4%)	3 (8.8%)	2 (14.3%)

Values are presented as median and interquartile ranges (IQR) or n (%).

ACE=angiotensin-converting enzyme; ARB=angiotensin-II receptor blocker; BMI = body mass index; CAD= coronary artery disease; CABG=coronary artery bypass grafting; PCI = percutaneous coronary intervention.

**Table 2:**

Comparison between global MBF and MFR estimates obtained with  $^{99m}\text{Tc}$ -sestamibi SPECT and  $^{13}\text{N}$ -ammonia PET with and without spline fitting

Standard OSEM reconstruction			
	$^{99m}\text{Tc}$ -sestamibi SPECT (N=30)	$^{13}\text{N}$ -ammonia (N=30)	p-value
Global rest flow (mL/g/min)	0.80 (0.57-1.07)	0.73 (0.62-0.83)	0.17
Global corrected rest flow (mL/g/min)	0.85 (0.73-0.95)	0.93 (0.70-1.04)	0.84
Global stress flow (mL/g/min)	1.74 (1.22-2.48)	1.45 (1.22-1.67)	0.017
Global MFR	2.15 (1.69-2.94)	1.90 (1.68-2.21)	0.082
Corrected global MFR	2.05 (1.54-2.54)	1.66 (1.26-2.07)	0.012
Rest CVR (mL/min/g/mmHg)	123.1 (103.5-161.7)	115.0 (105.9-141.1)	0.11
Stress CVR (mL/min/g/mmHg)	52.3 (40.7-81.8)	63.9 (51.0-79.7)	0.34
Spline fitting reconstruction			
	$^{99m}\text{Tc}$ -sestamibi SPECT (N=21)	$^{13}\text{N}$ -ammonia (N=21)	p-value
Global rest flow (mL/g/min)	0.58 (0.47-0.71)	0.73 (0.60-0.83)	0.003
Global corrected rest flow (mL/g/min)	0.69 (0.56-0.74)	0.96 (0.68-1.06)	0.001
Global stress flow (mL/g/min)	1.28 (0.88-1.50)	1.44 (1.21-1.80)	0.024
Global MFR	2.20 (1.61-2.46)	1.90 (1.71-2.23)	0.4
Corrected global MFR	1.72 (1.50-2.44)	1.55 (1.22-2.08)	0.073
Rest CVR (mL/min/g/mmHg)	175.7 (133.0-203.1)	117.8 (102.1-151.3)	<0.001
Stress CVR (mL/min/g/mmHg)	80.2 (62.2-94.03)	62.6 (50.4-84.4)	0.002

Myocardial blood flow (MBF) is reported in mL/min/g. Myocardial flow reserve (MFR) was calculated as the ratio between stress MBF and that at rest. Coronary vascular resistance (CVR) was calculated as the ratio between mean arterial blood pressure and MBF, and reported as mmHg/ml/min/g.

\* P-values refer to the comparison between SPECT and PET groups and are based on the Wilcoxon signed-rank test.

SPECT: single photon emission computed tomography; PET: positron emission tomography



**Table 3:**

Analyses of reproducibility for global MBF and MFR

Standard OSEM reconstruction (N=12)					
	1 <sup>st</sup> SPECT	2 <sup>nd</sup> SPECT	p-value	Mean difference between paired SPECT scans	Mean percentage difference (%)
Global rest flow (mL/min/g)	0.85 (0.52-1.07)	0.70 (0.56-1.04)	0.76	0.048±0.36	3.1%
Corrected rest flow (mL/min/g)	0.89 (0.73-1.29)	0.89 (0.68-1.42)	0.75	0.054±0.48	5.0%
Stress flow (mL/min/g)	1.65 (1.03-2.69)	1.61 (1.19-2.04)	0.81	0.028±0.63	2.6%
Global MFR	2.19 (1.59-2.48)	2.08 (1.78-2.59)	0.84	0.01±0.76	0.7%
Corrected global MFR	1.60 (1.19-2.46)	1.98 (1.22-2.47)	1.00	-0.04±0.87	2.6%
Spline fitting reconstruction (N=14)					
	1 <sup>st</sup> SPECT	2 <sup>nd</sup> SPECT	p-value	Mean difference between paired SPECT scans	Mean percentage difference (%)
Global rest flow (mL/min/g)	0.64 (0.51-0.80)	0.62 (0.54-0.86)	0.46	-0.029±0.17	4.6%
Corrected rest flow (mL/min/g)	0.71 (0.68-0.82)	0.74 (0.64-0.88)	0.14	-0.057±0.19	6.6%
Stress flow (mL/min/g)	1.52 (1.02-1.73)	1.13 (1.00-1.95)	0.73	0.014±0.42	1.4%
Global MFR	2.21 (1.76-2.46)	1.83 (1.71-2.40)	0.51	0.12±0.73	5.6%
Corrected global MFR	1.73 (1.40-2.39)	1.65 (1.36-2.12)	0.59	0.14±0.52	7.6%

Myocardial flow reserve (MFR) is calculated as the ratio between stress myocardial blood flow (MBF) and that at rest.

\* P-values refer to the comparison between two paired SPECT scans performed within 2 weeks and are based on the Wilcoxon signed-rank test. Mean percentage difference (%) was calculated as absolute change in value divided by the average of the two sequential SPECT measurements, multiplied by 100.

SPECT: single photon emission computed tomography.